

Forecasting Sea Levels for 2050 and Its Relationship With Environmental Variables With Time Series Models

Martha Elva Ramírez Guzmán, and Erick Javier Suárez Sánchez

Colegio de Postgraduados, Mexico

Abstract: The World Meteorological Organization (WMO) cautions that 2024 is poised to become the warmest year on record, fueled by the El Niño phenomenon. This persistent trend, continuing from 2023, is projected to trigger droughts, off-season tropical storms, and rising sea levels, imperiling 40% of the global population residing within 100 kilometers of coastlines. Historical data reveal alarming sea level rises: 1.7 cm/year in the 20th century, 3.1 cm/year in its final two decades, and 3.7 ± 0.5 cm/year since 2006, primarily driven by global warming, glacier melting, and thermal expansion. This study introduces a statistical methodology linking sea level rise with temperature and pollution time series. Notable insights include: sea level exhibits a constant, positive trend over time, with 48% annual growth following La Niña events. Global temperature increases sea level with a three-month delay. CO₂ levels impact sea levels with a similar three-month lag. GARCH modeling reveals volatile sea level behavior. By 2050, the model predicts a 31 cm sea level rise. This research underscores the effectiveness of statistical methodologies in understanding natural phenomena and making predictions, as well as the urgent need for climate action to mitigate the impacts of rising sea levels and associated climate risks.

Key words: sea level, SARIMA, transfer function, GARCH

1. Introduction

Sea level measurement is crucial for understanding the impacts of climate change, managing coastal resources, and ensuring the safety of communities worldwide. Rising sea levels pose significant threats to coastal ecosystems, infrastructure, and human settlements. In particular, sea level rise is a key indicator of global warming, helping scientists track the effects of climate change [1]. Also, accurate sea level data informs coastal management and flood protection strategies, safeguarding communities and infrastructure [2]. With respect to ecosystem conservation, changes in it, affect coastal ecosystems, including salt marshes, mangroves, and coral reefs, which support biodiversity and fisheries [3].

Rising sea levels threaten the livelihoods and homes of millions, particularly in low-lying coastal areas, which means human migration and displacement [4].

Also, sea level rise affects tourism, fisheries, and coastal development, with estimated annual costs exceeding \$100 billion [5]. There are several possible causes of rising sea levels, some of them are thermal expansion (as the Earth's atmosphere warms, oceans expand and contract less), contributing to sea level rise, glacier melting, large eruptions, which can cause temporary sea level changes [1] and human activities which produce CO₂ emissions, thought mining and industrial activities [6, 7]. Therefore, this research was motivated to analyze the behavior of monthly sea level from December 1992 to November 2022 as well as the effect of global and ocean temperature along with CO₂, which reflects the human activities on the sea level.

2. Material and Methods

To quantify the impacts of human activities, specifically CO₂ emissions, global temperature, and ocean temperature, on sea level rise, this study employs seasonal ARIMA, transfer function, and GARCH models. These time series models, introduced by Box

Corresponding author: Martha Elva Ramírez Guzmán, Ph.D.. E-mail: martharg@colpos.mx.

and Jenkins [8], offer a streamlined alternative to more complex geophysical models, such as Ocean General Circulation Models (OGCMs) [9] and geoid models [10].

2.1 Seasonal Multiplicative ARIMA Model

A multiplicative Seasonal *ARIMA* model is denoted as $(p, d, q)(P, D, Q)[s]$, where p : Order of the autoregressive (*AR*) component, d : Order of non-seasonal differencing, q : Order of the moving average (*MA*) component, P : Order of the seasonal autoregressive (*SAR*) component, D : Order of seasonal differencing, Q : Order of the seasonal moving average (*SMA*) component and s : Seasonal periodicity. The general form of the multiplicative seasonal *ARIMA* model is:

$$\Phi_P(B^s)\phi_p(B)(1-B)^d(1-B^s)^D y_t = \theta_Q(B^s)\theta_q(B)a_t$$

where: $\Phi_P(B^s)$: Seasonal autoregressive polynomial of order P , $\phi_p(B)$: Non-seasonal autoregressive polynomial of order p , $\theta_q(B)$: Non-seasonal moving average polynomial of order q , $\theta_Q(B^s)$: Seasonal moving average polynomial of order Q , B : Backshift operator, y_t : dependent time series and a_t : white noise error term.

2.2 Transfer Function Model

A Box-Jenkins transfer function model (ARIMAX):

$$y_t = c + \sum_{i=1}^p \phi_i y_{t-i} + \sum_{j=1}^q \theta_j a_{t-j} + \sum_{k=0}^b \beta_k x_{t-k} + a_t$$

where:

y_t : Dependent time series at time t .

x_t : Exogenous time series at time t .

c : Constant term.

ϕ_i : Autoregressive coefficients (AR).

θ_j : Moving average coefficients (MA).

β_k : Coefficients of the exogenous variable.

a_t : White noise error term.

p : Order of the autoregressive component.

q : Order of the moving average component.

b : Maximum lag of the exogenous variable.

is used to model the relationship between a dependent time series and an exogenous time series.

2.3 GARCH Model

Generalized Autoregressive Conditional Heteroskedasticity Model (GARCH), is a statistical framework used to analyse and forecast financial time series that exhibit volatility clustering. These models capture the phenomenon of volatility clustering, where large variable of interest movements are followed by large variable of interest movements, and small variable of interest movements are followed by small variable of interest movements.

In this particular case, a *GARCH* model is used to estimate the volatility of the error term of an *ARIMA* model, which gives an idea of the variability that sea level presents over time. A *GARCH* model incorporates autoregressive components of the variance (σ^2), which captures the persistence of volatility, and square error components (a_t^2), which represents random deviations. The *GARCH*(q, p) model is defined as:

$$\begin{aligned} a_t &= \mu + \epsilon_t \\ \epsilon_t &= \sigma_t z_t \\ \sigma_t^2 &= \alpha_0 + \sum_{i=1}^q \alpha_i \epsilon_{t-i}^2 + \sum_{j=1}^p \beta_j \sigma_{t-j}^2 \end{aligned}$$

y_t : value of the series at time t .

μ : mean of the series.

ϵ_t : error term at time t .

σ_t^2 : conditional variance at time t .

z_t : white noise term (typically assumed to follow a standard normal distribution). α_0 , α_i , and β_j are the parameters of the model.

3. Results and Discussion

3.1 Series Description

The data were obtained from the National Oceanic and Atmospheric Administration (NOAA) by three distinct satellites from December 1992 to November

2022. The satellites were TOPEX/Poseidon, Jason-1, Jason-2, and Jason-3 [2]. These measurements were averaged to obtain monthly global sea level increase.

Descriptive statistics of 360 observations from December 1992 to November 2022 showed almost symmetrical distribution given that the median was similar to the mean (Table 1). Sea level data consisted of measured changes in centimetres of the sea surface level, compared to the average sea level measured from 1993 to 2008. This period serves as a stable reference period, minimizing the impact of interannual variability and climate patterns like El Niño-Southern Oscillation (ENSO), also this period coincided with the launch of satellite altimetry missions (TOPEX/Poseidon, Jason-1, and Jason-2), providing consistent and accurate sea level data [2]. The

1993-2008 average establishes a climate normal, allowing for comparison of subsequent sea level changes [2]. Global and ocean temperatures were taken as well from NOAA [2]. Researchers often use the period from 1910 to 1990 as a reference for measuring exceedance of global or oceanic temperature, because early 20th-century marks the beginning of widespread temperature records, providing a century-long perspective. 1910 is relatively close to the pre-industrial era (1850-1900), allowing researchers to study climate change since the Industrial Revolution, which had less anthropogenic influence. Besides, period 1910-1990 was relatively stable, with minimal volcanic eruptions and solar variability and global temperature records [11, 12].

Table 1 Descriptive statistics of the variables (December 1992 to November 2022).

Variable	Mean	Median	Min	Max	Standard Deviation	Skewness	Kurtosis
Y_t : Sea level (cm)	2.42	2.06	-25.98	84.28	2.74	0.29	-0.97
X_{1t} : Global temperature (°C)	0.67	0.67	0.07	1.35	0.23	0.13	-0.16
X_{2t} : Ocean temperature (°C)	0.50	0.50	0.18	0.87	0.15	0.18	-0.78
X_{3t} : CO ₂ (ppm)	384.73	383.65	354.44	418.58	18.08	0.16	-1.15

3.2 Structural Changes of Sea Level

Sea Level Variations from December 1992 to November 2022, relative to the 1993-2008 mean (Fig. 1A), shows five level changes. These changes in sea level increases and become more frequent as time goes long. The duration of them were 9 (December 1992-June 2001), 7 (July 2001-August 2008), 6 (September 2008-July 2014), 4 (August 2014-August 2018) and 4 years (September 2018-November 2022). Respective mean sea levels were: -0.7160032 (December 1992-June 2001), 1.4037035 (July 2001-August 2008), 3.0893561 (September 2008-July 2014), 5.2148205 (August 2014-August 2018) and 6.8581797 (September 2018-November 2022). Fig. 2B, also shows three slopes change: 0.02 (December 1992-December 2010), 0.05 (January 2011-December 2016) and 0.04 (January 2017-November 2022).

Interestingly, the latter two slopes exhibit a more pronounced incline compared to the first, indicating an acceleration in the rate of sea level change over time. The results mean that sea level presented a positive and constant trend over time, with a growth rate of 48% ($= 0.04 \times 12 \times 100$) annually and that after the appearance of the phenomenon known as “La Niña”, although a decline was experienced, subsequently the slope of sea level increased.

3.3 Train and Test Data

Sea level original data was divided in train and test data in order to test the quality of the ARIMA modelling. Train set included data from December 1992 to November 2016, and from December 2016 to November 2022 for the test set. Model (1) shows the SARIMA model adjusted to train data.

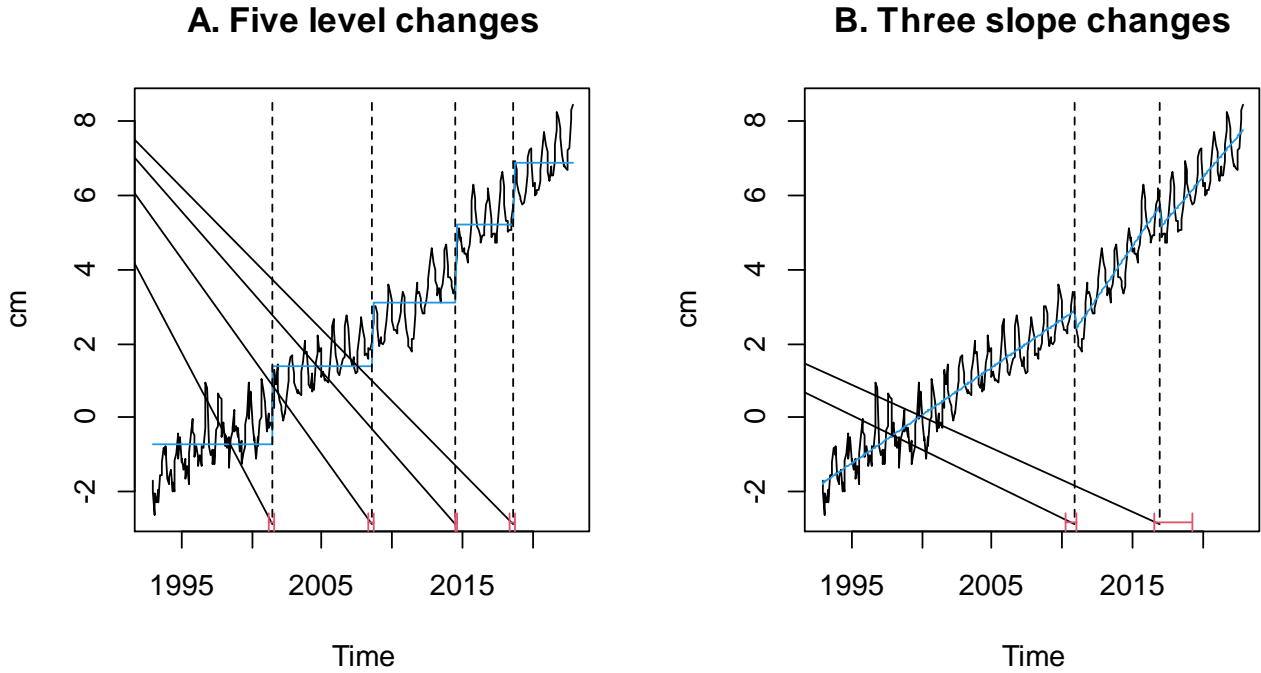


Fig. 1 (A) Sea level increase, and (B) slope of sea level increase, derived from a stable reference period spanning 1993 to 2008.

$$(1 + 0.33B^{12})(1 + 0.70B)(1 - B^{12})(1 - B) y_t = a_t$$

$$a_t \sim N(0, 0.087)$$

$$BIC = 128.15 \quad (1)$$

Model (1) took into account the stochastic trend and the seasonal behaviour of the series and suggested that sea level time series exhibits a moderate positive yearly autocorrelation and strong positive autocorrelation at lag 1. It is noteworthy, that 95 % confidence level (C.L.)

of this model contains the test time series (Fig. 2). As was expected, 95% (C.L.) gets wider as time goes by. Fig. 2, also shows the annual sea level mean of 3.7 ± 0.5 cm, which was estimated by the IPCC [1]. This mean was estimated from monthly data from 2006 to 2018. Therefore, SARIMA(1,1,0)(1,1,0) [12] was good model to represent the seasonal increase of sea level.

y_t : ARIMA (1,1,0)(1,1,0)[12] forecast v.s. Test data

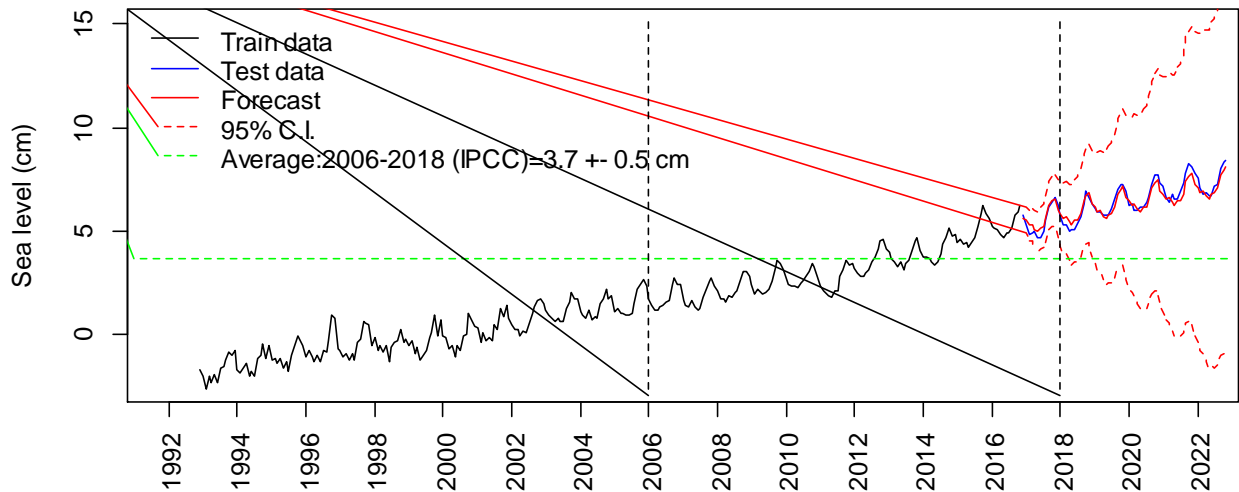


Fig. 2 Seasonal ARIMA forecast and test data from December 2022.

3.4 Volatility Analysis of Sea Level

An analysis of the residuals of model (1) detected an additive outlier in the observation 49 (December 1996), which coincided with a major EL Niño [3]. This outlier was incorporated in model 2 as:

$$\begin{aligned} (1 + 0.35B^{12})(1 - 0.70B)(1 - B^{12})(1 - B)y_t \\ = -1.17I_t + a_t \\ a_t \sim N(0, 0.085) \end{aligned} \quad (2)$$

Volatility clustering and leptokurtosis presented in the squared residuals of model (2) were taken into account by the GARCH ($q = 1, p = 0$) model:

$$\sigma_t^2 = 0.0012 + 0.55\epsilon_t^2 \quad (3)$$

with a skew parameter = 8.27 and skew normal distribution (Fig. 3A). Constant term (0.0012): represents the minimum volatility level, indicating a baseline risk or uncertainty. ARCH term ($0.55\epsilon_t^2$) measured the impact of past errors (ϵ_t) on current

variability. A high coefficient (0.55) indicates strong persistence of shocks, meaning past large errors lead to increased volatility. The absence of a GARCH term ($p = 0$) suggested that lagged volatility does not directly influence current volatility. Skew Parameter (8.27) indicates significant skewness in the distribution, with a positive value suggesting right-skewness and substantial asymmetry to the right, this implies more extreme increases of sea level in the long term. The residuals of model (3) did not rejected H_0 : Residuals has normal distribution, with a p -value = 0.12 (Fig. 3B). This GARCH model provides valuable insights into the underlying volatility dynamics and distributional characteristics of the sea level, enabling more informed decision-making. By combining ARIMA and GARCH models, this approach accounts for linear (SARIMA) and nonlinear patterns (GARCH).

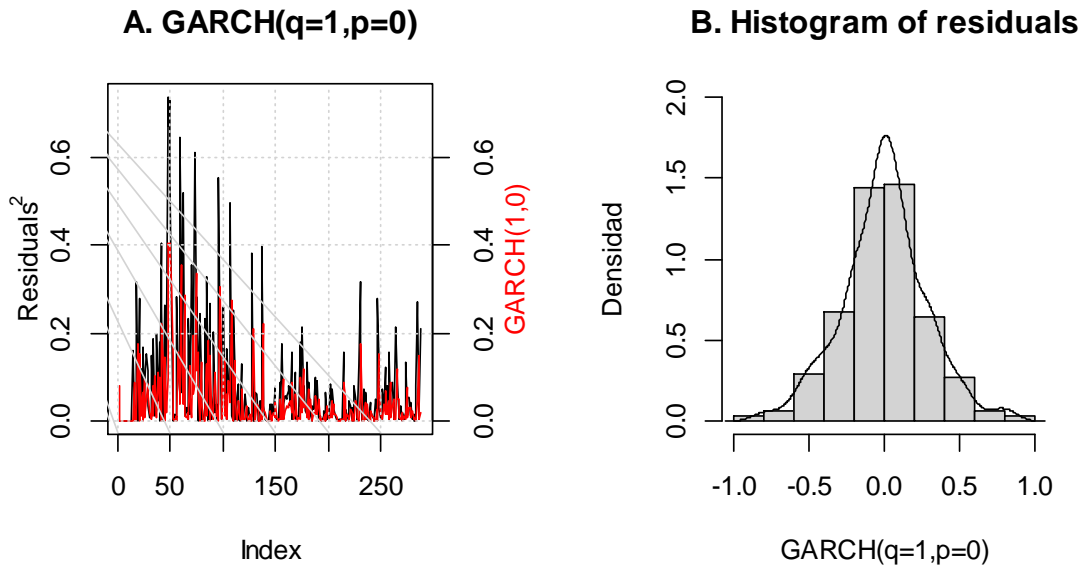


Fig. 3 (A) Squared residuals of model (2) in black and the GARCH($q = 1, p = 0$), which is model (3) adjusted to the squared residuals of model (2) in red color. (B) Residuals of model 3.

3.5 Transfer Function Analysis

The four time series (from December 1992 to November 2022) presented an increase trend (Fig. 4). Therefore, all the time series contained an integrated term of order 1 ($d = 1$). Besides, sea level (Y_t) and

CO_2 (Y_{3t}) showed a seasonal behaviour (Fig. 4), therefore seasonal terms were included in these models (Table 2). We observed that global temperature (X_{1t}) and ocean temperature (X_{2t}) depend of the previous three months and one month, respectively. In other

words, global temperature is more persistent than ocean temperature.

We employed individual transfer functions to model the relationships between sea level (Y_t) and its drivers: global temperature (X_{1t}), ocean temperature (X_{2t}), and CO_2 (X_{3t}). This approach allowed for: clearer

interpretation of the physical mechanisms underlying each relationship, avoidance of multicollinearity issues, capture of unique dynamics between each input and output, more parsimonious models and better goodness-of-fit compared to a combined model.

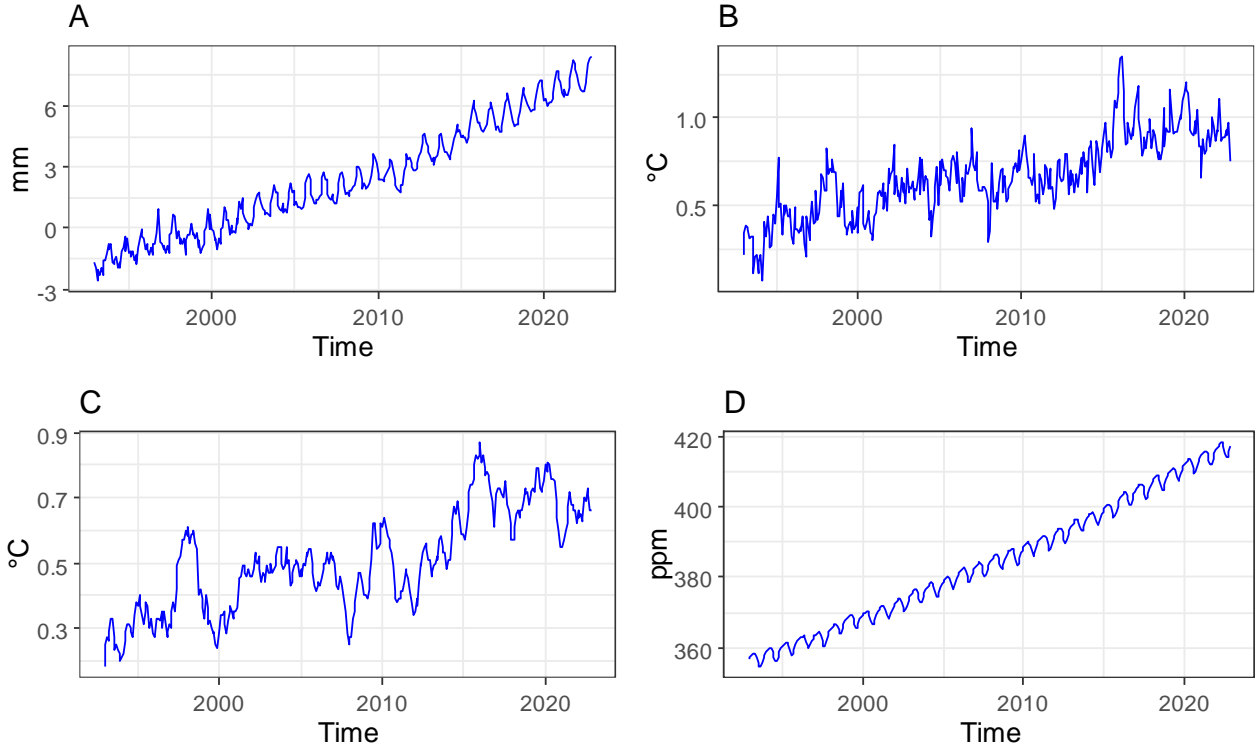


Fig. 4 (A) Sea level time series. (B) Global temperature. (C) Ocean temperature. (D) CO_2 . Data are from December 1992 to November 2022.

Cross correlation functions of pairs of residuals series: (Y_t^*, X_{1t}^*) , (Y_t^*, X_{2t}^*) and (Y_t^*, X_{3t}^*) , presented significant “peaks”. The “peaks” and form of the crosscorrelation functions of the pairs mentioned, produced the next transfer function models:

$$\begin{aligned} &\text{Transfer function between } Y_t \text{ and } X_{1t}: \\ &(1 + 0.36B^{12})(1 + 0.65B)(1 - B^{12})(1 - B)Y_t \\ &= \frac{0.37}{(1 + 0.76)}X_{1t} - 1.46I_t + a_t \\ &\sigma_{a_t}^2 = 0.076 \end{aligned} \quad (4)$$

$$\begin{aligned} &\text{Transfer function between } Y_t \text{ and } X_{2t}: \\ &(1 + 0.35B^{12})(1 + 0.68B)(1 - B^{12})(1 - B)Y_t \\ &= 0.82X_{2t-3} - 1.46I_t a_t \\ &\sigma_{a_t}^2 = 0.076 \end{aligned} \quad (5)$$

Transfer function between Y_t and X_{3t} :

$$\begin{aligned} &(1 + 0.36B^{12})(1 + 0.68B)(1 - B^{12})(1 - B)Y_t \\ &= 0.13X_{3t-3} - 0.112X_{3t-5} \\ &- 1.28I_t + a_t \\ &\sigma_{a_t}^2 = 0.076 \end{aligned} \quad (6)$$

Models 4, 5, and 6 required the inclusion of an intervention variable, it, to account for an anomalous event in December 1996. This variable was defined as: $I_t = 1$ if $t = \text{December 1996}$ and $I_t = 0$ otherwise. The December 1996 event had a one-time negative impact and it could be caused by a weaker La Niña during October and November of 1996, before a major El Niño which occurred from 1996-1997 [8].

Presence of the intervention variable I_t produce a symmetrical distribution of the residuals.

Interpretation of model (4): In this model, $0.37/(1 + 0.76B)$ represents the dynamic relationship between global temperature (X_{1t}) and sea level (Y_t). The numerator indicates contemporary increase in sea level of 0.37 cm for an increase in 1°C in global temperature, while the denominator represents the rate of decrease of global temperature effect on sea level. The steady state gain was 0.21 ($0.21 = 0.37/(1 + 0.76)$), it indicates that, in the long run, a 1-unit increase in global temperature will result in a 0.21 cm increase in sea level.

Interpretation of Model (5): The 3-month lag represent the time it takes for ocean temperature changes to affect sea level. The strong relationship between ocean temperature and sea level suggests that oceanic processes play a significant role in sea level variability.

Interpretation of Model (6): Sea level responds to CO_2 changes with both positive and negative lagged effects. The positive effect (0.13) at 3 months, suggests a short-term increase in sea level due to CO_2 . The negative effect (-0.112) at 5 months suggests a subsequent decrease in sea level. The lagged effects may represent the time it takes for CO_2 changes to affect sea level through thermal expansion, ice melting, or ocean circulation changes.

The opposing effects at different lags suggest complex interactions between CO_2 and sea level.

Seasonal components indicated that sea level is influenced by climate cycles. Analysis of residuals of models: 4, 5 and 6 produce symmetric distributions (Fig. 5). Also absence of autocorrelation with the Ljung and Box test [13] was not rejected with p-values: 0.642, 0.642 and 0.59, for global temperatura, ocean temperatura and CO_2 , respectively.

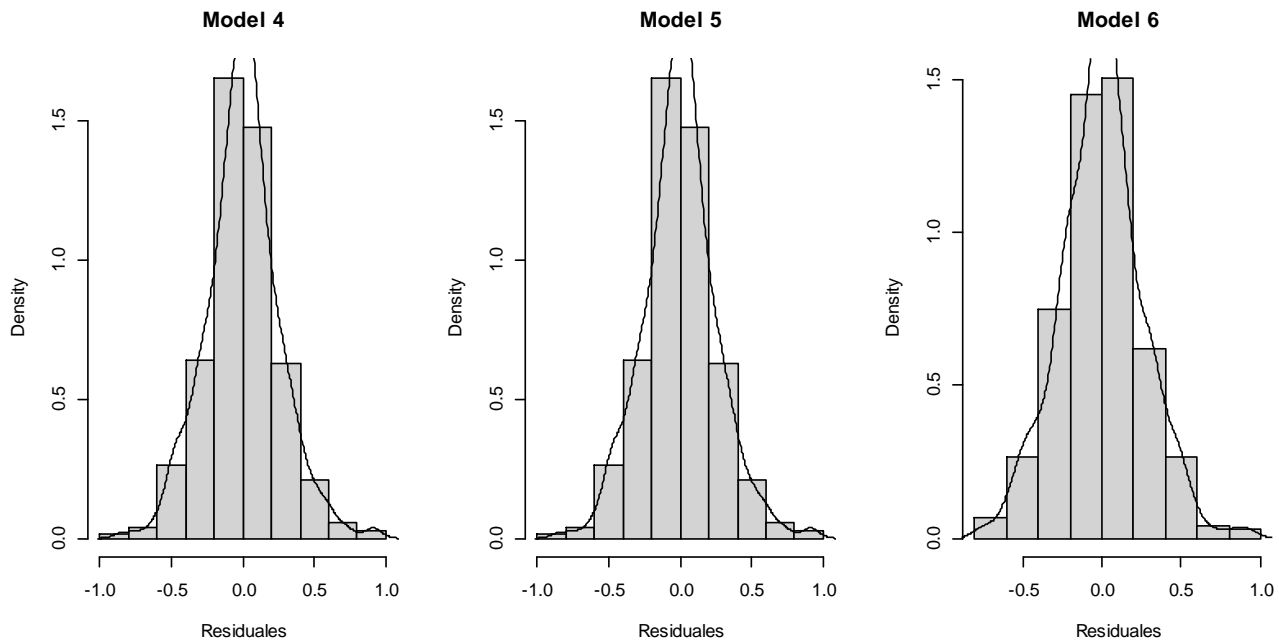


Fig. 5 Residuals of transfer function models.

3.6 Annual Average Prediction for 2050

In order to estimate the annual average prediction sea level for 2050, model: ARIMA(1,1,0)(1,1,0) [12] was applied for the whole data (December 1992 to November 2022) (Table 2).

This model produced an annual average prediction for 2050 of 30.57 cm. The IPCC [1] forecasted an average of 28 cm. As we can see both forecasts are very similar.

Table 2 Parameter estimates of the ARIMA models adjusted to sea level and environmental time series from December 1992 to November 2022.

Model	Variable	AR1	AR2	AR3	MA1	SAR1	$\sigma_{a_t}^2$
ARIMA(1,1,0)(1,1,0) [12]	Y_t : Sea level	-0.68	-	-	-	-0.35	0.078
ARIMA(3,1,0)	X_{1t} : Global temperature	-0.41	-0.16	-0.20			0.010
ARIMA(1,1,0)	X_{2t} : Sea temperature	0.14	-	-	-	-	0.001
ARIMA(0,1,1)(0,1,1)[12]	X_{3t} : CO_2	-	-	-	-0.79	0.86	0.015

4. Conclusion

Sea level rise accelerated over time, with durations of: 9, 7, 6, 4, and 4 years for the periods: December 1992-June 2001, July 2001-August 2008, September 2008-July 2014, August 2014-August 2018 and September 2018-November 2022, respectively. The corresponding average levels were: 0, 1.40, 3.09, 5.21, and 6.85 cm, respectively.

Three positive growth changes were observed in the series' slope, highlighting an accelerated sea level rise from January 2017. The predictive series showed positive slopes and correlated positively with sea level change. This analysis showed that sea level time series tend to react to changes in environmental variables within few months. This statement reflects the widely accepted scientific consensus on the relationship between climate change and sea level rise.

Transfer function model fitting revealed that for every 1°C increase in ocean temperature, sea level rises by 0.82 cm. Global temperature has a positive impact on sea level with a contemporaneous impact of around 0.37 cm which increase at a rate of 76%. Sea level responds to CO_2 changes with both positive and negative lagged effects. The positive effect (0.13) at 3 months suggests a short-term increase in sea level due to CO_2 . The negative effect (-0.112) at 5 months suggests a subsequent decrease in sea level. The lagged effects may represent the time it takes for CO_2 changes to affect sea level through thermal expansion, ice melting, or ocean circulation changes. The opposing effects at different lags suggest complex interactions between CO_2 and sea level.

The application of time series methods offers a remarkably efficient and accessible approach to analyzing climate change indicators, such as sea level rise, outperforming more intricate non-linear models like physical models. This breakthrough unlocks new avenues for predictive analysis and insightful decision-making.

References

- [1] IPCC, *Climate Change: The Physical Science Basis. Contribution of Working Group I to the Fifth Assessment Report of the Intergovernmental Panel on Climate Change*, Chapter 12.3, Cambridge University Press, 2021.
- [2] National Oceanic and Atmospheric Administration (NOAA), *Sea Level Rise Technical Report*. (2022)
- [3] IPCC, *Climate Change 2001: The Scientific Basis. Contribution of Working Group I to the Third Assessment Report of the Intergovernmental Panel on Climate Change*, edited by Houghton, J. T., Y. Ding, D. J. Griggs, M. Noguer, P. J. van der Linden, X. Dai, K. Maskell, and C.A. Johnson, Cambridge University Press, Cambridge, United Kingdom and New York, NY, USA, 2001, pp. 13-30.
- [4] United Nations, *Surging seas in a warming world: The latest science on present-day impacts and future projections of sea-level rise*, 2021, available online at: https://www.un.org/sites/un2.un.org/files/slr_technical_brief_26_aug_2024.pdf.
- [5] UNHCR, The UN Refugee Agency, *Focus area strategy plan for climate action 2024-2030*, available online at: https://reporting.unhcr.org/climate-action-focus-area-strategy-plan-2024-2030?_gl=1*1lmxizu*_gcl_au*ODk3NzU1MzgyLjE3MjkxOTkyODI.*_rup_ga*Mzc0MTE3NzgxLjE3MjkxOTkyODI.*_rup_ga_EVDQTJ4LjE3MjkxOTkyODI.*_ga_50TI4Mi4xLjAuMTcyOTE5OTI4Mi42MC4wLjA.*_ga*Mzc0MTE3NzgxLjE3MjkxOTkyODI.*_ga_X2YZPJ1XWR*MTcyOTE5OTI4Mi4xLjAuMTcyOTE5OTI4Mi42MC4wLjA.
- [6] OECD, *Development Co-operation Report: Tackling Poverty and Inequalities through the Green Transition*, OECD Publishing, Paris, available online at:

- https://www.oecd.org/en/publications/development-co-operation-report-2024_357b63f7-en.html.
- [7] United Nations Environment Programme, Emissions Gap Report 2023: Broken Record — Temperatures hit new highs, yet world fails to cut emissions (again), 2023, Nairobi, available online at: <https://wedocs.unep.org/bitstream/handle/20.500.11822/43922/EGR2023.pdf?sequence=3&isAllowed=y7>.
- [8] Box, George E. P., Gwilym M. Jenkins, Gregory C. Reinsel, and Greta M. Ljung, *Time Series Analysis: Forecasting and Control* (5th ed.), Hoboken, NJ: John Wiley & Sons, 2016, pp. 395-469.
- [9] J. E. Kay, , C. Deser, A. Phillips, A. Mai, C. Hannay, G. Strand, J. M. Arblaster, S. C. Bates, G. Danabasoglu, J. Edwards, M. Holland, P. Kushner, J.-F. Lamarque, D. Lawrence, K. Lindsay, A. Middleton, E. Munoz, R. Neale, K. Oleson, L. Polvani, and M. Vertenstein, The community earth system model (CESM) large ensemble project: A community resource for studying climate change in the presence of internal climate variability, *Bulletin of the American Meteorological Society* 96 (2015) (8): 1333-1349, doi: 10.1175/BAMS-D-13-00255.1.
- [10] M. E. Tamisiea, E. M. Hill, R. M. Ponte, J. L. Davis, I. Velicogna, and N. T. Vinogradova, Impact of self-attraction and loading on the annual cycle in sea level, *Journal of Geophysical Research: Oceans* 115 (2010) (C7) C07004, doi: 10.1029/2009JC005687.
- [11] David B. Enfield, Evolution and historical perspective of the 1997-1998 El Niño-Southern Oscillation Event, *Bulletin of Marine Science*, 1998.
- [12] Michelle L. L'Heureux, Ken Takahashi, Andrew B. Watkins, Anthony G. Barnston, Emily J. Becker, Tom E. Di Liberto, Felicity Gamble, Jon Gottschalck, Michael S. Halpert, Boyin Huang, Kobi Mosquera-Vásquez, and Andrew T. Wittenberg, Observing and predicting the 2015/16 El Niño, *Bulletin of the American Meteorological Society* 98 (2017) (7): 1363-1382, doi: 10.1175/BAMS-D-16-0009.1.
- [1] G. M. Ljung, and G.E.O. Box, On measure of lack of fit in time series models, *Biometrika* 65 (1978) (2): 297-303.